

Reflection high-energy electron diffraction measurements of reciprocal space structure of 2D materials

Y Xiang, F-W Guo, T-M Lu and G-C Wang

Department of Physics, Applied Physics and Astronomy, and Center for Materials, Devices, and Integrated Systems, Rensselaer Polytechnic Institute, 110 8th Street, Troy, NY 12180-3950, USA

E-mail: xiangy@rpi.edu

Received 15 August 2016, revised 26 September 2016

Accepted for publication 3 October 2016

Published 31 October 2016



CrossMark

Abstract

Knowledge on the symmetry and perfection of a 2D material deposited or transferred to a surface is very important and valuable. We demonstrate a method to map the reciprocal space structure of 2D materials using reflection high energy diffraction (RHEED). RHEED from a 2D material gives rise to 'streaks' patterns. It is shown that from these streaks patterns at different azimuthal rotation angles that the reciprocal space intensity distribution can be constructed as a function of momentum transfer parallel to the surface. To illustrate the principle, we experimentally constructed the reciprocal space structure of a commercial graphene/SiO₂/Si sample in which the graphene layer was transferred to the SiO₂/Si substrate after it was deposited on a Cu foil by chemical vapor deposition. The result reveals a 12-fold symmetry of the graphene layer which is a result of two dominant orientation domains with 30° rotation relative to each other. We show that the graphene can serve as a template to grow other materials such as a SnS film that follows the symmetry of graphene.

Keywords: RHEED, 2D materials, graphene, reciprocal space

(Some figures may appear in colour only in the online journal)

1. Introduction

2D materials have been extensively studied in recent years because of their many novel and unusual electronic and optoelectronic properties [1, 2]. Common 2D materials include graphene, hexagonal boron nitride, and transition metal dichalcogenides. When a 2D material is grown on a surface, it may form many different 2D textures including single crystal, random polycrystalline, or a texture with a preferred in-plane orientation. Often roughness can also exist in the 2D materials. Structural characterization of these 2D materials is of great importance. A most direct quantitative and statistical way to detect the symmetry and perfection of the 2D materials is by electron diffraction, in particular, low-energy electron diffraction (LEED) [3]. The electron energy used is from tens of eV to hundreds of eV. Typically in LEED, electrons are incident normally onto the surface of the 2D materials and the reflected diffraction pattern would reveal the symmetry and perfection of the 2D lattice. The diffraction

pattern is close (not exactly) to represent the 2D reciprocal space lattice structure. However, LEED is very sensitive to charging effect. If the substrate holding the 2D material is not conductive, then the diffraction pattern is either distorted or disappears altogether unless a flood gun is used.

An alternative electron diffraction technique that is complementary to LEED but more tolerant of the charging effect of non-conductive samples is reflection high energy diffraction (RHEED) [4]. In RHEED, electron energy ranging from several keV to tens of keV is used. Depending on the substrate used, the charging effect on the integrity of the diffraction pattern can be reduced substantially. A good common example is a 2D material on an oxide layer on a Si substrate. If the oxide layer thickness is on the order of tens of nm to hundreds of nm, RHEED can give an excellent diffraction pattern while LEED may not. However, in a conventional RHEED configuration, the electrons are incident at a glancing angle with respect to the surface and the diffraction pattern only provides limited information on the reciprocal

lattice structure. RHEED pole figure technique [5] was a newly developed tool for near surface texture characterization of 3D thin films or nanostructures using the transmission mode. This technique is used to measure the 3D crystal orientation distribution near the surface but not applicable to 2D materials. For 2D materials, RHEED patterns are collected using reflection mode. In this paper, we show that it is possible to obtain the entire reciprocal space structure of a 2D material by rotating the sample around the surface normal and measuring the RHEED patterns as a function of the azimuthal angle. Azimuthal RHEED has been employed to map the reciprocal space structure of a sample [6–8] to study surfaces and thin film in the past. Here, we use this method to construct the reciprocal space structure of a 2D graphene sheet on SiO₂/Si. All 2D structures with limited long-range order produce ‘streaks’ in a RHEED pattern. A 2D reciprocal space structure is constructed by measuring the characteristics of streaks as a function of momentum transfer parallel to the surface while varying the azimuthal angle.

2. RHEED 2D texture analysis

First, we consider a single crystal 2D material. The 3D reciprocal space structure of a single crystal 2D material consists of vertical ‘rods’ [4]. Figure 1(a) shows a schematic of the 3D reciprocal space structure of a 2D hexagonal lattice. We label the momentum transfer $\mathbf{k} = \mathbf{k}_o - \mathbf{k}_i$, where \mathbf{k}_i and \mathbf{k}_o are the incident and outgoing wave vectors, respectively. The \mathbf{k} in the x , y , and z directions are denoted as k_x , k_y , and k_z , respectively. The diffraction intensity along the k_z direction is uniform and featureless. In RHEED, the wave vector of electrons is large for an incident beam energy ranging from several keV to tens of keV and the Ewald sphere cuts through the rods as shown in figure 1(b). Streaks would form in the RHEED diffraction pattern as shown in figure 1(c), when looking into the $-k_x$ direction. The 2D reciprocal space structure can be obtained by looking into the $-k_z$ direction as shown in figure 1(d). Experimentally, this can be constructed by plotting the RHEED streak intensity as a function of the momentum transfer parallel to the surface while varying the in-plane azimuthal angle.

If a 2D material consists of grains with random in-plane orientations as shown in figure 2(a), then the 3D reciprocal space structure will be a set of concentric cylinders around k_z axis with different radii as shown in figure 2(b). The RHEED diffraction pattern will show streak-like intensity distribution that resembles figure 2(c). By looking into the $-k_z$ direction, the 2D reciprocal space structure consists of a set of rings with different radii as shown in figure 2(d).

The two types of 2D materials presented above, a single crystal and a polycrystalline film, are extreme cases. Perhaps the more interesting case is a 2D film that is neither single crystal nor random polycrystalline. In this case, the 2D reciprocal space structure of this 2D material contains broken rings and has a preferred in-plane orientation.

3. RHEED from graphene/SiO₂/Si

3.1. Experimental

Graphene is perhaps the most well-known 2D layered material. It has been actively researched and possesses many remarkable electronic and optoelectronic properties [9]. Graphene on SiO₂/Si (or other substrates) is commercially available. Typically it is grown by chemical vapor deposition (CVD) technique on a Cu foil [10] and then transferred to a SiO₂/Si substrate [11, 12]. Since the Cu foil is not a single crystal, the nucleation of graphene at different regions on the Cu foil would possess different orientations. The net result is that the graphene grown on the Cu foil is polycrystalline in nature. However, it was shown that the orientation of the graphene grains is not completely random. In fact, the grains often show two dominant orientations with a 30° rotation with respect to each other and each orientation exhibits an angular spread [13]. The structure we analyzed is a commercially available graphene film (graphene-supermarket.com). This is a film grown by CVD on a Cu foil and then transferred to a SiO₂(~88 nm)/Si substrate. The dimension of this graphene sample is 1 cm × 1 cm. Figures 3(a) and (b) show the scanning electron microscopy (SEM, ZEISS SUPRA 55) and atomic force microscopy (AFM, PSI XE100) images, respectively. The images were taken from different places of the graphene. Both SEM and AFM images show a dominant single layer graphene with a small number of bi-layer graphene islands on top of a continuous layer of graphene. The thickness of the bi-layer island is about 8.4 Å from an AFM line scan along the white dashed line indicated in figure 3(b). Grain boundaries and wrinkles [14] of graphene are obvious in both images.

The graphene/SiO₂/Si sample was loaded into the RHEED chamber without any prior treatment. The RHEED system consists of an electron gun (model RDA-003G) which generates a 20 keV electron beam incident at a glancing angle of ~1° on the sample surface. The emission current used was 45 μA. The RHEED pattern was projected on a phosphor screen mounted on a 6 inch flange which was about 20 cm away from the sample in a vacuum chamber with a base pressure of 10⁻⁸ Torr. The RHEED pattern was captured by a digital camera positioned outside the chamber facing the phosphor screen. The sample was mounted on a holder with the sample’s azimuthal rotation controlled by a stepper motor. In order to probe the entire upper half of the reciprocal space, the sample was rotated azimuthally with a 1.8° step size from 0° to 180° in 100 steps and the corresponding RHEED pattern was recorded at each incremental step [15].

3.2. Results

Figure 4(a) shows a typical RHEED pattern from the commercial graphene sample taken at a certain azimuthal angle (φ), which we defined as $\varphi = 0.0^\circ$. The scale bar was calibrated using the RHEED pattern of an epitaxial CdTe(100) film on a single crystal GaAs(100) substrate with a known lattice constant under the same experimental conditions [16].

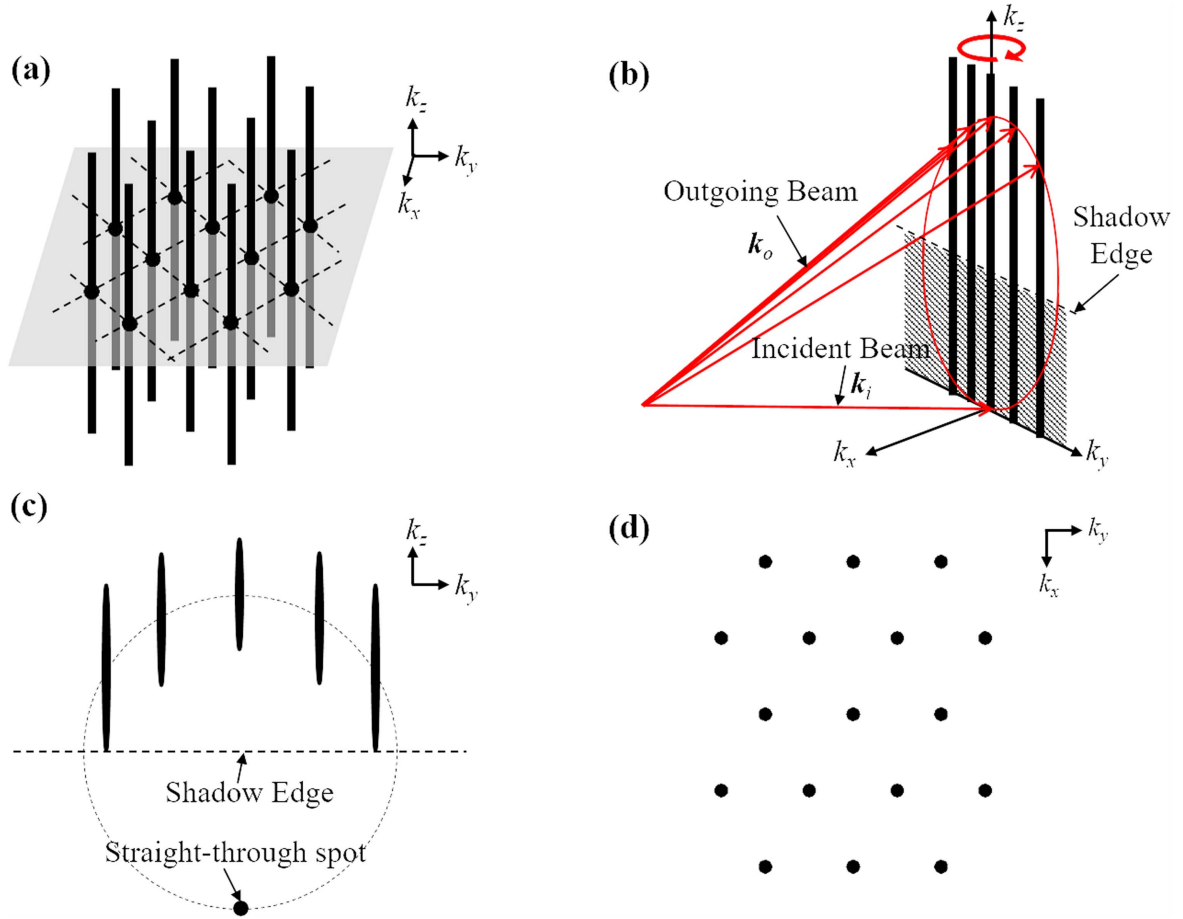


Figure 1. (a) A schematic of the reciprocal space structure of a 2D hexagonal lattice, (b) a schematic showing how the Ewald sphere cuts through the reciprocal rods. The curly red arrow represents the rotation around the sample normal direction at various azimuthal angle φ , (c) a simulated RHEED pattern, and (d) a schematic of the 2D reciprocal space structure of a 2D hexagonal lattice looking into the negative k_z direction.

The pattern shows a strong broad streak at the center and two weak streaks at the left side and right side of the center streak. The two axes in the yellow coordinate system shown in figure 4(a) indicate the directions of k_{\perp} and k_{\parallel} , where $k_{\perp} \equiv k_z$ and $k_{\parallel} \equiv (k_x^2 + k_y^2)^{1/2}$, $k_x = k \sin \varphi$ and $k_y = k \cos \varphi$. The origin is chosen to be the straight through spot. The inset in figure 4(a) is the intensity line scan along the k_{\perp} axis, showing that the intensity along the k_{\perp} axis is continuous beyond the shadow edge. For our graphene sample, the vertical distance between two graphene layers determined by an AFM line scan at the edge of a bi-layer graphene island is 8.4 \AA . This means that the intensity would oscillate with a period of $0.75 \text{ \AA}^{-1} \left(= \frac{2\pi}{8.4 \text{ \AA}} \right)$ and be suppressed at $k_{\perp} = i \times 0.37 \text{ \AA}^{-1}$ (where i is an odd number) if there is a substantial contribution of electron diffraction from the bilayer graphene islands [17]. However, we did not observe such oscillation. This indicates that the diffraction intensity is dominated by the single layer graphene.

In order to analyze quantitatively the peak position and width of each streak shown in figure 4(a), we imported the RHEED patterns into the software ImageJ to extract the

intensity profile. We assume the diffraction intensity distribution function in figure 4(a) is $f(k_{\parallel}, k_{\perp})$. Running a marco program written in ImageJ Marco Language, we obtained the normalized intensity $I'(k_{\parallel})$ as a function of k_{\parallel} through the following relation:

$$I'(k_{\parallel}) = \frac{\int_{k_{\perp}^a}^{k_{\perp}^b} f(k_{\parallel}, k_{\perp}) dk_{\perp}}{\int_{k_{\perp}^a}^{k_{\perp}^b} f(k_{\parallel}^{\max}, k_{\perp}) dk_{\perp}}, \quad (k_{\perp}^a \leq k_{\parallel} \leq k_{\perp}^b), \quad (1)$$

where k_{\parallel}^{\max} is the k_{\parallel} position that maximizes the integral $\int_{k_{\perp}^a}^{k_{\perp}^b} f(k_{\parallel}, k_{\perp}) dk_{\perp}$. Specifically, the labeled positions k_{\perp}^a , k_{\perp}^b , k_{\parallel}^a and k_{\parallel}^b in figure 4(a) are chosen to be 1.8 \AA^{-1} , 9.1 \AA^{-1} , -13.0 \AA^{-1} and 13.0 \AA^{-1} , respectively. The intensity is integrated along the k_{\perp} axis in order to improve the signal-to-noise ratio. The reason that we can use the integral is that the diffraction intensity mainly comes from a single layer graphene and the reciprocal rods of a single layer graphene are continuous and featureless along the k_{\perp} axis. Since the intensity profile in principle should be symmetric about the k_{\perp} axis, a linear background intensity is subtracted from $I'(k_{\parallel})$ (normalized to 1) to correct the experimental uncertainty.

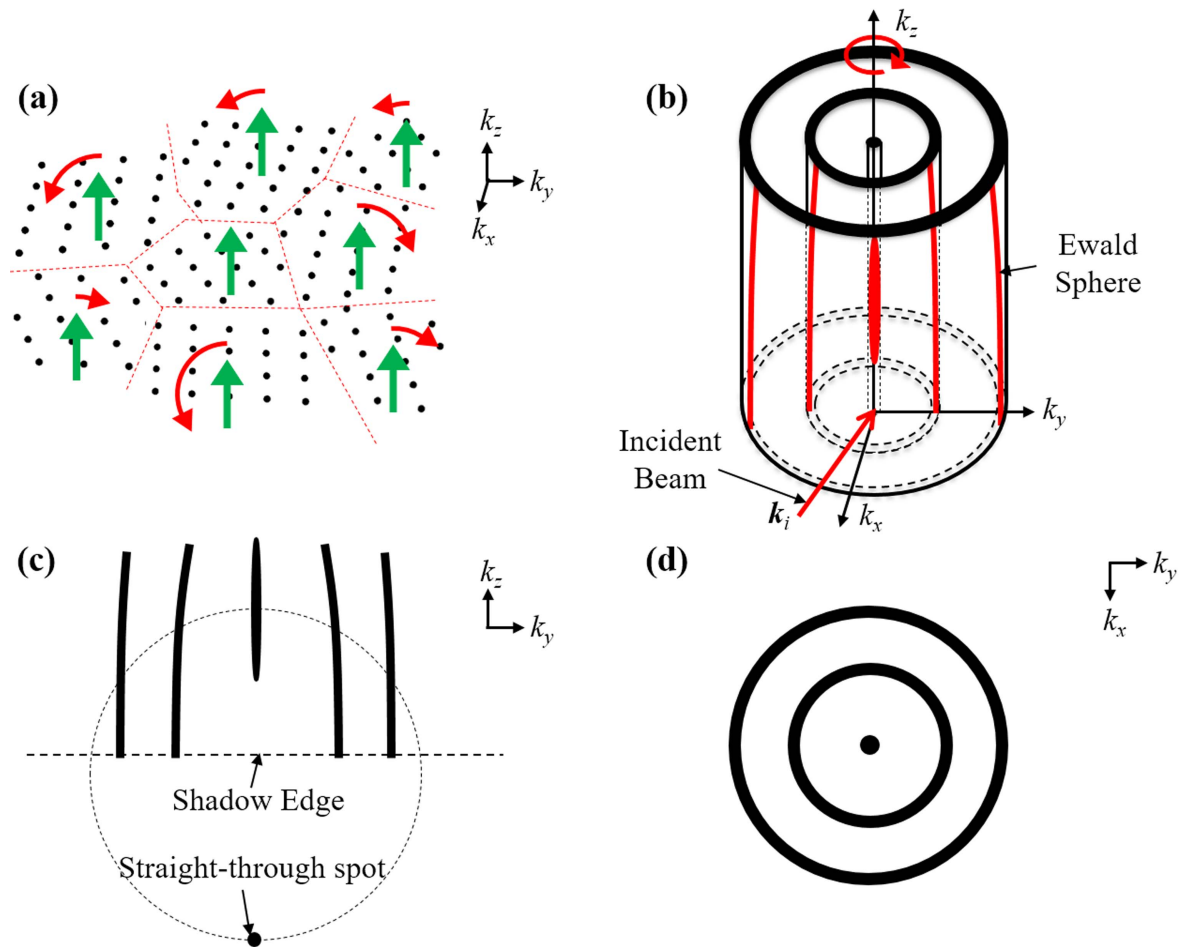


Figure 2. (a) A schematic of the real space structure of a 2D material consisted of randomly oriented grains. The curved red arrows represent random rotated grains and the straight up pointing green arrows represent the direction perpendicular to the substrate. (b) A schematic showing the 3D reciprocal space structure of the 2D material and how it cuts through the Ewald sphere, the curly red arrow represents the rotation around the sample normal direction at various azimuthal angle φ . (c) A simulated RHEED pattern, and (d) a schematic of the 2D reciprocal space structure of the 2D material with randomly oriented grains.

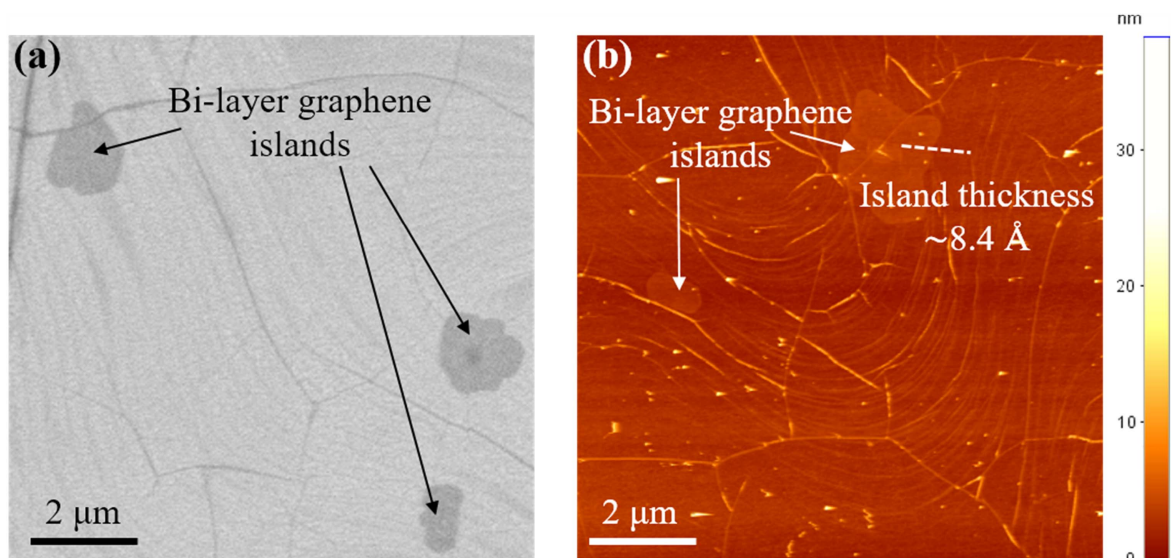


Figure 3. (a) An SEM image and (b) an AFM image showing different areas of the graphene surface. The arrows in both figures indicate bi-layer graphene islands. The z-scale bar indicating the surface height in the AFM image is shown on the right side of AFM image. The AFM line scan is represented by a white dashed line in (b). The darker wavy lines in (a) and brighter wavy lines in (b) are grain boundaries. The faint wavy lines in (a) and (b) are wrinkles in graphene.

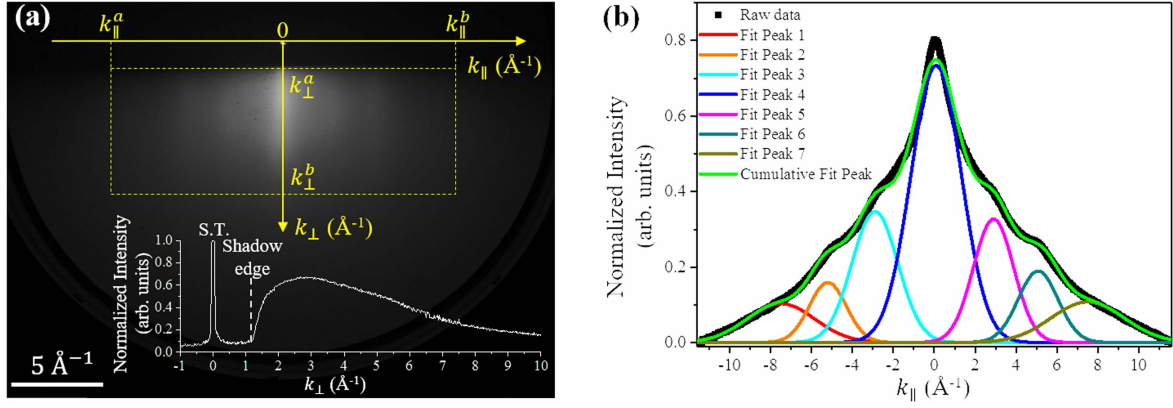


Figure 4. (a) A RHEED pattern collected from a commercial graphene sample with the 20 keV electron beam incident at $\varphi = 0.0^\circ$. The yellow coordinate system is centered at the straight through (S.T.) spot. The k_{\parallel} axis and k_{\perp} axis are parallel and perpendicular to the shadow edge, respectively. The inset in (a) shows an intensity line scan along the k_{\perp} axis. The black squares in (b) show the experimentally measured intensity along the k_{\parallel} axis, $I(k_{\parallel})$. The seven fit peaks and the cumulative fit peak are plotted in different colors. The peak number and the corresponding color are shown in the legend.

Table 1. Theoretical prediction of peak positions and experimentally measured peak positions and FWHMs of peaks.

(hk)	Theoretical $ \vec{G}(hk) $ (\AA^{-1})	Experimental peak position (\AA^{-1})	Experimental FWHM (\AA^{-1})
$(\bar{2}\bar{1})$	7.790	-7.5 ± 0.2	3.9 ± 0.3
$(\bar{2}0)$	5.889	—	—
$(\bar{1}\bar{1})$	5.100	-5.2 ± 0.1	2.1 ± 0.1
$(\bar{1}0)$	2.944	-2.9 ± 0.1	2.7 ± 0.2
(00)	0	0.1 ± 0.1	2.9 ± 0.1
(10)	2.944	2.9 ± 0.1	2.3 ± 0.1
(11)	5.100	5.1 ± 0.1	2.3 ± 0.2
(20)	5.889	—	—
(21)	7.790	7.5 ± 0.2	4.2 ± 0.3

Then we obtain $I(k_{\parallel})$:

$$I(k_{\parallel}) = I'(k_{\parallel}) - \left[\frac{I'(k_{\parallel}^b) - I'(k_{\parallel}^a)}{k_{\parallel}^b - k_{\parallel}^a} k_{\parallel} - \frac{I'(k_{\parallel}^b)k_{\parallel}^a - I'(k_{\parallel}^a)k_{\parallel}^b}{k_{\parallel}^b - k_{\parallel}^a} \right], \quad (k_{\parallel}^a \leq k_{\parallel} \leq k_{\parallel}^b). \quad (2)$$

The raw data points (black squares) in figure 4(b) show the intensity profile $I(k_{\parallel})$ obtained experimentally. The raw data points can be fitted using seven Gaussians. The seven fit peaks and the cumulative fit peak are also plotted in different colors in figure 4(b). The RHEED diffraction pattern shown in figure 4(a) is actually made up of seven broad streaks. Theoretical prediction and experimental result of the peak positions are listed in table 1. Graphene has a hexagonal lattice with a lattice constant $a_0 = 2.464 \text{ \AA}$. $\vec{G}(hk)$ is the reciprocal space lattice vector associated with the Miller index (hk) and its magnitude $|\vec{G}(hk)| = \frac{4\pi}{\sqrt{3}a_0} \sqrt{h^2 + hk + k^2}$. The peak positions and full-width-at-half-maximum (FWHM)s are obtained from the Gaussian fits of the peaks. The peak broadening is a result of a combined effect of the orientational angular spreads and the wrinkles (roughness) of the graphene layer [17]. The $(\bar{2}0)$ is missing because the reciprocal distance

($\sim 0.8 \text{ \AA}^{-1}$) between $(\bar{2}0)$ and $(\bar{1}\bar{1})$ is much smaller than the average FWHM ($> 2 \text{ \AA}^{-1}$) of these streaks. According to the Rayleigh criterion for the resolution limit [18], we would not be able to resolve them. The same argument applies to the absence of the (20) peak.

For a single crystal graphene, however, (00), (10) and (11) are not collinear points in the reciprocal space. The planar-like Ewald sphere would not cut through them simultaneously at any azimuthal angle. The fact that they show up at the same time in a single RHEED pattern leads us to conclude that the graphene sample is not a single crystal. To study the in-plane orientation distribution of the graphene grains, we constructed the experimental 2D reciprocal space structure for this sample. The 2D reciprocal space structure is the cross-section view of the reciprocal space by looking into the $-k_{\perp}$ direction. It is constructed by plotting the intensity as a function of k_{\parallel} at different φ . At each φ , an intensity profile $I_{\varphi}(k_{\parallel})$ similar to that shown in figure 4(b) is extracted from the corresponding RHEED pattern. Plotting the azimuthal-dependent intensity profile $I_{\varphi}(k_{\parallel})$ in a polar coordinate system with the radius being k_{\parallel} and the polar angle being φ , and representing the intensity by different colors, we get the 2D reciprocal space structure of this graphene sample as shown in figure 5(a).

The most striking feature of figure 5(a) is the circularly wavy contours at $k_{\parallel} \approx 5 \text{ \AA}^{-1}$ that exhibit 12 approximately evenly-spaced peaks. For a single crystal graphene, theoretically there should be only six peaks, whose (hk) indices are (11), $(\bar{1}2)$, $(\bar{2}1)$, $(\bar{1}\bar{1})$, $(1\bar{2})$, $(2\bar{1})$, at $k_{\parallel} = 5.1 \text{ \AA}^{-1}$. The existence of 12 peaks confirms that the graphene is not a single crystal. The 12 peaks can be explained if we assume that the graphene has two dominant orientations with a 30° rotation with respect to each other. To illustrate this point, a theoretical model of the 2D reciprocal space structure is presented in figure 5(b). The cyan spots are the 2D reciprocal lattice points of single crystal graphene and the yellow spots are rotated 30° from the cyan spots around the k_{\perp} axis. This theoretical model consists of a (00) spot at the center, the

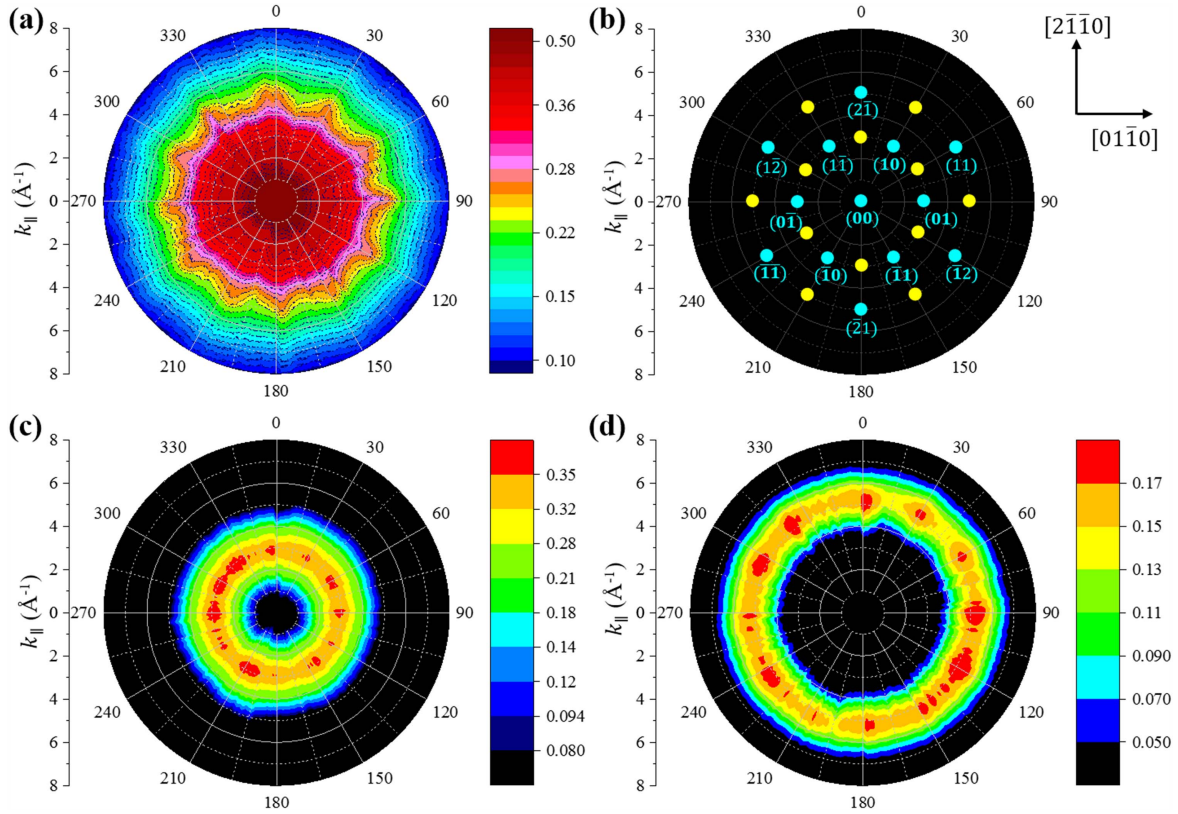


Figure 5. (a) The RHEED 2D reciprocal space structure measured from the commercial graphene sample. (b) The theoretical 2D reciprocal space structure of the graphene layer. The cyan spots are 2D reciprocal lattice points of a single crystal graphene with the corresponding (hk) indices labeled. The yellow spots are rotated 30° from the cyan spots around the rotation axis which is the k_x direction. $k_x = k_{\parallel} \sin \varphi$ and $k_y = k_{\parallel} \cos \varphi$. The arrows on the right side indicate the in-plane directions for graphene, $[2\bar{1}\bar{1}0]$ and $[01\bar{1}0]$ along $\varphi = 0^\circ$ and 90° , respectively. (c) and (d) show the $I(k_{\parallel}, \text{inner})$ and $I(k_{\parallel}, \text{outer})$ plotted in polar coordinate system. These intensity distributions of the inner peaks and outer peaks are extracted from the RHEED 2D reciprocal space structure in (a).

inner 12 spots at $k_{\parallel} = 2.9 \text{ \AA}^{-1}$ and the outer 12 spots at $k_{\parallel} = 5.1 \text{ \AA}^{-1}$. The twelve peaks of the contour lines in figure 5(a) match well with the outer 12 spots in figure 5(b). However, the inner spots in figure 5(b) are not obviously seen in figure 5(a) due to overlapping with the high intensity of the center peak.

At every azimuthal angle φ , the intensity profile $I_{\varphi}(k_{\parallel})$ can be decomposed into seven Gaussian profiles by doing multiple peak fit similar to that in figure 4(b). That is:

$$I_{\varphi}(k_{\parallel}) = \sum_{i=1}^7 I_i(k_{\parallel}). \quad (3)$$

The center positions of the Gaussian profiles $I_1(k_{\parallel})$ to $I_7(k_{\parallel})$ range from about -7.5 to about 7.5 \AA^{-1} . $I_2(k_{\parallel})$ and $I_6(k_{\parallel})$ constitute the outer peaks in figure 5(a) while $I_3(k_{\parallel})$ and $I_5(k_{\parallel})$ constitute the inner peaks which are not obvious in figure 5(a). That is:

$$I_{\varphi}(k_{\parallel}, \text{outer}) = I_2(k_{\parallel}) + I_6(k_{\parallel}), \quad (4)$$

$$I_{\varphi}(k_{\parallel}, \text{inner}) = I_3(k_{\parallel}) + I_5(k_{\parallel}). \quad (5)$$

Plotting $I(k_{\parallel}, \text{inner})$ and $I(k_{\parallel}, \text{outer})$ in a similar way as in figure 5(a), we obtain figures 5(c) and (d), respectively. In this way, we can present the intensity contributions from the inner

and the outer peaks separately from the combined intensity shown in figure 5(a).

In both figures 5(c) and (d), we observed some localized intensities on a continuous ring. The positions of those localized intensities in figures 5(c) and (d) match the theoretical inner 12 spots and the theoretical outer 12 spots shown in figure 5(b), respectively. This leads to a qualitative picture on the grain orientation of the commercial graphene sample. That is, some of the graphene grains are randomly oriented while others prefer to orient with a 30° rotation with respect to each other. This is consistent with the results from transmission electron microscopy (TEM) analyses of a CVD grown graphene suspended on TEM grid by Huang *et al* [13].

4. Graphene as a template to grow epitaxial SnS film

The preferred in-plane orientation in the graphene layer can have a profound impact on the materials epitaxially grown on it. We deposited a ~ 527 nm thick SnS film on the commercial graphene substrate using thermal evaporation. The substrate was heated and maintained at 280°C during the evaporation. Figure 6(a) shows an SEM cross section view of the SnS film on graphene/SiO₂/Si. The texture of the SnS film was characterized by x-ray pole figure (Bruker D8 Discover) taken

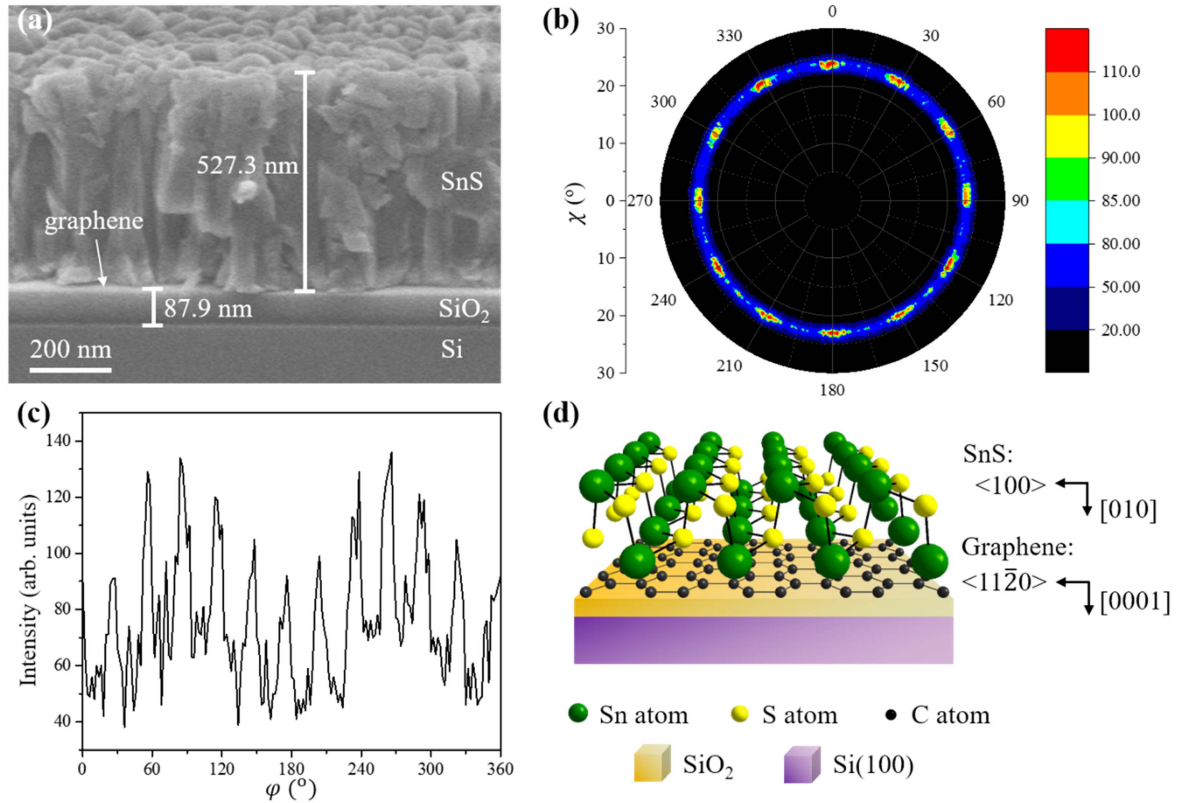


Figure 6. (a) An SEM cross section view of the SnS film epitaxially grown on the graphene/SiO₂/Si substrate. The graphene layer between SnS and SiO₂ is not visible in the SEM image. (b) The measured x-ray {160} pole figure from the SnS/graphene/SiO₂/Si sample presented in χ angle and azimuthal angle φ . The out-of-plane direction of the SnS film is [010]. The range of χ in the plot is from 0° to 30° that covers the 12 poles located at $\chi = 23.321^\circ$. (c) An azimuthal scan of the x-ray intensity at $\chi = 23.321^\circ$ shows 12 evenly spaced peaks. (d) A schematic of the parallel epitaxy of SnS on the graphene/SiO₂/Si sample showing the orientation domain of SnS and the epitaxy relationship.

at $2\theta = 53.443^\circ$, which is presented in figure 6(b). Peaks from Si substrate that show up due to tungsten contamination in the x-ray tube have been subtracted from the original data in figure 6(b). Note that a pole figure [19] is different from a 2D reciprocal space structure in that the radial axis is the angle χ rather than k_{\parallel} . The χ angle ranges from 0° to 90° with 0° and 90° being the normal and parallel directions to a substrate, respectively. Both x-ray pole figure and 2D reciprocal space structure characterize the in-plane orientation distribution of the films. Figure 6(b) shows the {160} pole figure of the SnS film that has the [010] out-of-plane. Twelve evenly spaced {160} poles on a continuous ring at χ angle = 23.321° were observed. Figure 6(c) is a phi scan of the 12 poles at $\chi = 23.321^\circ$. Comparing this x-ray pole figure result to the constructed RHEED 2D reciprocal space structures shown in figures 5(c) and (d), we conclude that the SnS was epitaxially grown on the graphene surface through van der Waals forces. The SnS grains orient parallel to the two dominant graphene grains which have 30° rotation with respect to each other. This result is compared to a recent report on the epitaxial growth of SnS on CVD grown bi-layer graphene that was transferred from a Cu foil [20], which also showed a 12-fold dominant poles in the phi scan of the {160} pole figure. Figure 6(d) is a schematic showing the epitaxy

relationship between the SnS film and the graphene layer. That is, $[010]_{\text{SnS}} // [0001]_{\text{graphene}}$ for the out-of-plane direction and $\langle 100 \rangle_{\text{SnS}} // \langle 11\bar{2}0 \rangle_{\text{graphene}}$ for the in-plane direction.

5. Conclusion

We present a method to construct the reciprocal space structure of 2D materials using RHEED. The diffraction patterns were obtained at different in-plane azimuthal angle φ of the sample by rotating the sample with respect to the surface normal. At each in-plane angle, the intensity is expressed as a function of momentum transfer parallel to the substrate k_{\parallel} . The reciprocal space structure is therefore represented by the intensity distribution $I(k_{\parallel})$ as a function of the momentum transfer parallel to the substrate for all in-plane azimuthal angle. We applied this method to a commercial single layer graphene. The measured intensity map reveals a 12-fold symmetry of graphene. The graphene layer is dominated by two orientation domains with a 30° rotation with respect to each other. This method does not require extensive 2D sample preparation and can be applied to other 2D materials. The graphene layer was used as a substrate to

grow an epitaxial SnS film and it is shown that the symmetry and orientation in the SnS film follow that of the graphene.

Acknowledgments

This project is supported by the National Science Foundation Award #DMR-1305293 and New York State Foundation of Science, Technology and Innovation through Focus Center-New York at Rensselaer Polytechnic Institute Award #C130117, Troy, New York. YX is supported by RPI Presidential Fellowship. We thank Y B Yang and A J Littlejohn for discussions.

References

- [1] Geim A K and Grigorieva I V 2013 Van der Waals heterostructures *Nature* **499** 419–25
- [2] Utama M I B, Zhang Q, Zhang J, Yuan Y, Belarfe F J, Arbiol J and Xiong Q 2013 Recent developments and future directions in the growth of nanostructures by van der Waals epitaxy *Nanoscale* **5** 3570–88
- [3] Robinson Z R, Tyagi P, Mowll T R, Ventrice C A Jr and Hannon J B 2012 Argon-assisted growth of epitaxial graphene on Cu (111) *Phys. Rev. B* **86** 235413
- [4] Ichimiya A and Cohen P I 2004 *Reflection High-Energy Electron Diffraction* (Cambridge: Cambridge University Press)
- [5] Wang G-C and Lu T-M 2014 *RHEED Transmission Mode and RHEED Pole Figures* (New York: Springer)
- [6] Braun W, Möller H and Zhang Y-H 1998 Reflection high-energy electron diffraction during substrate rotation: a new dimension for *in situ* characterization *J. Vac. Sci. Technol. B* **16** 1507–10
- [7] Satapathy D K, Jenichen B, Ploog K H and Braun W 2011 Azimuthal reflection high-energy electron diffraction study of MnAs growth on GaAs(001) by molecular beam epitaxy *J. Appl. Phys.* **110** 023505
- [8] Boschker J E, Momand J, Bragaglia V, Wang R, Perumal K, Giussani A, Kooi B J, Riechert H and Calarco R 2014 Surface reconstruction-induced coincidence lattice formation between two-dimensionally bonded materials and a three-dimensionally bonded substrate *Nano Lett.* **14** 3534–8
- [9] Allen M J, Tung V C and Kaner R B 2009 Honeycomb carbon: a review of graphene *Chem. Rev.* **110** 132–45
- [10] Li X *et al* 2009 Large-area synthesis of high-quality and uniform graphene films on copper foils *Science* **324** 1312–4
- [11] Liang X, Sperling B A, Calizo I, Cheng G, Hacker C A, Zhang Q, Obeng Y, Yan K, Peng H and Li Q 2011 Toward clean and crackless transfer of graphene *ACS Nano* **5** 9144–53
- [12] Li X, Zhu Y, Cai W, Borysiak M, Han B, Chen D, Piner R D, Colombo L and Ruoff R S 2009 Transfer of large-area graphene films for high-performance transparent conductive electrodes *Nano Lett.* **9** 4359–63
- [13] Huang P Y *et al* 2011 Grains and grain boundaries in single-layer graphene atomic patchwork quilts *Nature* **469** 389–92
- [14] Deng S and Berry V 2016 Wrinkled, rippled and crumpled graphene: an overview of formation mechanism, electronic properties, and applications *Mater. Today* **19** 197–212
- [15] Tang F, Parker T, Wang G and Lu T 2007 Surface texture evolution of polycrystalline and nanostructured films: RHEED surface pole figure analysis *J. Phys. D: Appl. Phys.* **40** R427
- [16] Chen L, Dash J, Su P, Lin C F, Bhat I, Lu T M and Wang G C 2014 Instrument response of reflection high energy electron diffraction pole figure *Appl. Surf. Sci.* **288** 458–65
- [17] Meyer J, Geim A, Katsnelson M, Novoselov K, Oberfell D, Roth S, Girit C and Zettl A 2007 On the roughness of single- and bi-layer graphene membranes *Solid State Commun.* **143** 101–9
- [18] Rayleigh L 1879 XXXI. Investigations in optics, with special reference to the spectroscope *Phil. Mag.* **8** 261–74
- [19] He B B 2011 *Two-Dimensional X-ray Diffraction* (Hoboken, NJ: Wiley)
- [20] Leung K K, Wang W, Shu H, Hui Y Y, Wang S, Fong P W, Ding F, Lau S P, Lam C-h and Surya C 2013 Theoretical and experimental investigations on the growth of SnS van der Waals epitaxies on graphene buffer layer *Cryst. Growth Des.* **13** 4755–9